TECHNICAL NOTE

Quantification of Protein A–Gold Staining for Peroxisomal Enzymes by Confocal Laser Scanning Microscopy

Naoko Ogiwara, Nobuteru Usuda, Masashi Yamada, Kohei Johkura, Kiyokazu Kametani, and Ayami Nakazawa

Department of Anatomy and Cell Biology (NO,NU,KJ,AN) and General Research Laboratory (KK), Shinshu University School of Medicine, Matsumoto, Japan, and Leica K.K. (MY), Tokyo, Japan

SUMMARY The protein A–gold technique has been widely applied for visual localization and quantification of various antigens by electron microscopy. Observation of specimens stained by the protein A–gold technique with conventional light microscopy is difficult because of insufficient sensitivity of the staining. Light microscopic visualization and quantification of the reaction products were attempted employing a confocal laser scanning microscope (CLSM). Liver tissues of normal and peroxisome proliferator-treated rats were fixed and embedded in Lowicryl K4M resin. Ultrathin and thin sections were stained for catalase and a peroxisome-specific β-oxidation enzyme by the protein A–gold technique. Ultrathin sections were observed by electron microscopy and the labeling density for each enzyme was analyzed with an image analyzer. Thin sections were observed with a CLSM in the reflection mode and the intensity of the light reflection was analyzed under the same conditions for all specimens. A comparison of these two observation procedures was also attempted using liver tissues stained with various concentrations of the antibody for catalase. The intensity of the reflection for each, as observed by CLSM, correlated well with the labeling density observed by electron microscopy. CLSM made it possible to quantify and to directly observe protein A–gold staining at the light microscopic level.

(J Histochem Cytochem 47:1343–1349, 1999)

The protein A–gold technique has been widely used to visualize the localization of various antigens by electron microscopy, because of its high sensitivity and high image resolution (Faulk and Taylor 1971; Romano and Romano 1977; Roth et al. 1978,1981; Bendayan 1984). This procedure has the further advantage that quantification of gold particles as reaction products enables the amount of antigen to be estimated, particularly in the cellular fine structures (Bendayan et al. 1980,1983; Bendayan and Reddy 1982; Bendayan 1984; Beier and Fahimi 1985; Yokota et al. 1987; Beier et al. 1988; Usuda et al. 1988,1991a,b; Desjardins and Bendayan 1991). Light microscopic visualization of the reaction products is rather difficult because of the faint red color of the

staining with colloidal gold (Roth 1982). Silver intensification of the reaction makes clear visualization possible (Bendayan et al. 1980; Danscher and Nörgaard 1983; Holgate et al. 1983), but the intensification itself makes quantification difficult.

Confocal laser scanning microscopy (CLSM) is coming to be commonly used in the observation of various kinds of specimens, most commonly with fluorescence, and quantification of the fluorescent reaction products has also been attempted (Good et al. 1992; Larsen et al. 1994; Verschure et al. 1994; Asaka et al. 1998). Another representative example of the use of CLSM is as a reflectance microscope. Because CLSM provides higher resolution of images and stronger intensity of the reflection light of the laser beam than the usual reflectance microscopes employing ordinary light, a variety of other kinds of application to other kinds of reaction product is possible, e.g., cerium for oxidase reactions, DAB for peroxidase reaction, silver for intensification of immunogold staining, and silver

impregnation for neural tissue of Golgi impregnation (Robinson and Batten 1989,1990; Freire and Boyde 1990; Uriel et al. 1995; Woolf et al. 1996; Ito and Otsuki 1998; Sun et al. 1998). Direct visualization of immunogold staining has also been reported to be possible by CLSM in the reflection mode (Van den Pol 1989).

In this study, hepatic peroxisomes were used as the subject of observation by CLSM in the reflection mode. The peroxisome is a spherical cell organelle with a diameter of about 0.5–1.0 μm (de Duve and Baudhuin 1966; Fahimi 1969) containing specific enzymes, e.g., catalase, d-amino acid oxidase, urate oxidase, and fatty acid β-oxidation enzymes, including enoyl-CoA hydratase/3-hydroxy acyl-CoA dehydrogenase (PH) (Osumi and Hashimoto 1979a; Bendayan et al. 1983; Yokota et al. 1987; Usuda et al. 1991b; Hashimoto 1996). A group of chemicals called peroxisome proliferators, which include clofibrate and dioctyl-phthalate (DOP), cause a marked increase in the number and volume of peroxisomes in hepatocytes and in the amount of their enzymes (Hess et al. 1965; Osumi and Hashimoto 1979b; Usuda et al. 1988). The magnitude differs for each enzyme, for PH the most and for other enzymes less (Reddy et al. 1981; Nemali et al. 1988). In previous studies, administration of peroxisome proliferators made the density of the distribution of catalase decrease and that of PH increase compared with those of normal peroxisomes (Reddy et al. 1981; Nemali et al. 1988; Usuda et al. 1988). In this study we attempted visualization of the reaction products of the protein A–gold technique and quantification of the density of distribution of gold particles, employing specimens of liver tissues of rats fed normal or DOP-containing diets stained for these peroxisomal enzymes.

Materials and Methods

Tissue Preparation

Liver tissues of 14-week-old male Wistar rats, fed normal or 1% DOP-containing diets (Osumi and Hashimoto 1979b), were fixed by perfusion with a fixative of 4% paraformaldehyde/0.1% glutaraldehyde/100 mM sodium phosphate, pH 7.4, for 15 min and then by immersion for 2 hr. After rinsing in a cold solution consisting of 100 mM lysine/100 mM sodium phosphate, pH 7.4/150 mM sodium chloride and dehydration in a graded series of cold ethanol, they were embedded in Lowicryl K4M at −20C by UV polimerization (Roth et al. 1981).
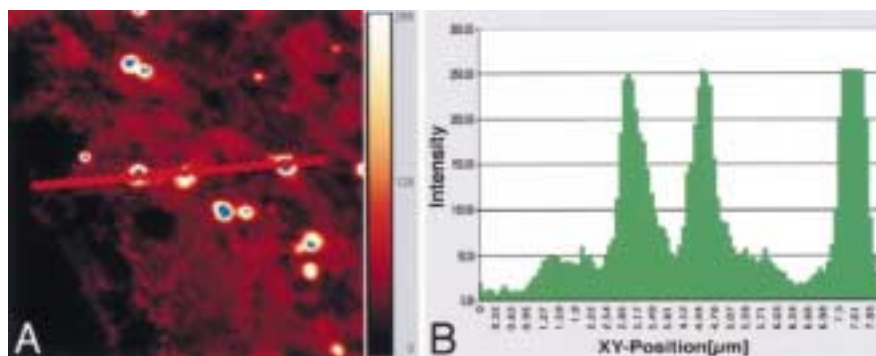
Immunoelectron Microscopy

Staining was performed as previously described (Usuda et al. 1988). Antibodies for rat liver catalase and PH were employed (Osumi and Hashimoto 1979a; Furuta et al. 1986). Sections of 0.1 μm were cut on a Dupont Sorvall MT2B ultramicrotome and mounted on Formvar membrane-coated nickel grids. The sections were soaked in 5 mg/ml bovine serum albumin in 50 mM Tris-HCl, pH 7.5/150 mM sodium chloride (TBS), containing 0.05% (v/v) Triton X-100 for 1 hr. They were then transferred to antibody solution (40 μg/ml of IgG in TBS containing 0.05 % Triton X-100 and 5 mg/ml of bovine serum albumin) and incubated for 1 hr at room temperature. After washing several times in TBS with 0.05% Triton X-100, the sections were transferred to a diluted solution of protein A–gold complex (15-nm gold particles) (EY Laboratories; San Mateo, CA) for 1 hr at a concentration of $A^{520} = 0.07$. The sections washed with the buffer solutions were then examined in a JEOL 1200 EX electron microscope at an accelerating voltage of 90 kV after staining with uranyl acetate and lead citrate.

Quantification of Gold Particles on Electron Micrographs

The labeling density, i.e., the number of gold particles per unit area of peroxisomes, was estimated for each enzyme in hepatocytes in the pericentral area of hepatic lobules. The area of peroxisomes, the cytoplasm, and the number of gold particles on them were measured using the computer software Ultimage (Graftek;

Figure 1 The procedure for measuring the intensity of reflecting light from peroxisomes on the line (line intensity) on a normal liver tissue section stained for catalase by the protein A–gold technique. The intensity was graded at 256 levels, i.e., the highest value was defined as 255 and the lowest as 0. The intensity was imaged with pseudo-color gradation: blue (255); white; orange (128); red and black (0) (**A**). Original magnification × 6400. The values of the reflection light measured are also shown as a histogram (**B**).

Voisins le Bretonneux, France). Fifty peroxisomes photomicrographed at a magnification of ×20,000 were evaluated in each group. The total labeling index was calculated as volume density × labeling density for electron microscopic observation (Beier et al. 1988; Nemali et al. 1988; Usuda et al. 1988), and volume density × the intensity of light reflection for CLSM observation.

Confocal Laser Scanning Microscopy and Quantitative Measurement

One-μm sections were collected on aminopropyl-tri-ethoxysilene-coated glass slides. They were stained in the same solution and with the same incubation time as for immunoelectron microscopy. Specimens were examined with a confocal laser scanning microscope (TCS NT; Leica Lasertechnik, Heidelberg, Germany). The CLSM was equipped with an Ar–Kr laser having three major emission lines at wavelengths of 488 nm,

568 nm, and 647 nm. The 488-nm line was employed because the intensity of this line is the most sustainable. The reflecting light from the specimens at 488 nm was captured by a photomultiplier. The reflection light incidents of the images were digitized in 256 grades (2^8 grades), i.e., the reflection from the area of sinusoids was set to 0 and that from normal peroxisomes stained for catalase to 255, so that the values of all four groups fitted this range. Fifteen randomly selected lines under which 50 peroxisomes were present were evaluated in each group. The value for each peroxisome was obtained by subtracting the average of the cytoplasmic reflection from the peroxisomal reflection. Figure 1 shows an example of the procedure for measurement of the light reflection from a specimen stained by the protein A–gold technique. Figure 1A is a digitized image of normal liver tissue stained for catalase. The sinusoid, cytoplasm, and three intense signals are located under the line. Figure 1B shows the line intensity of the reflection light mea-
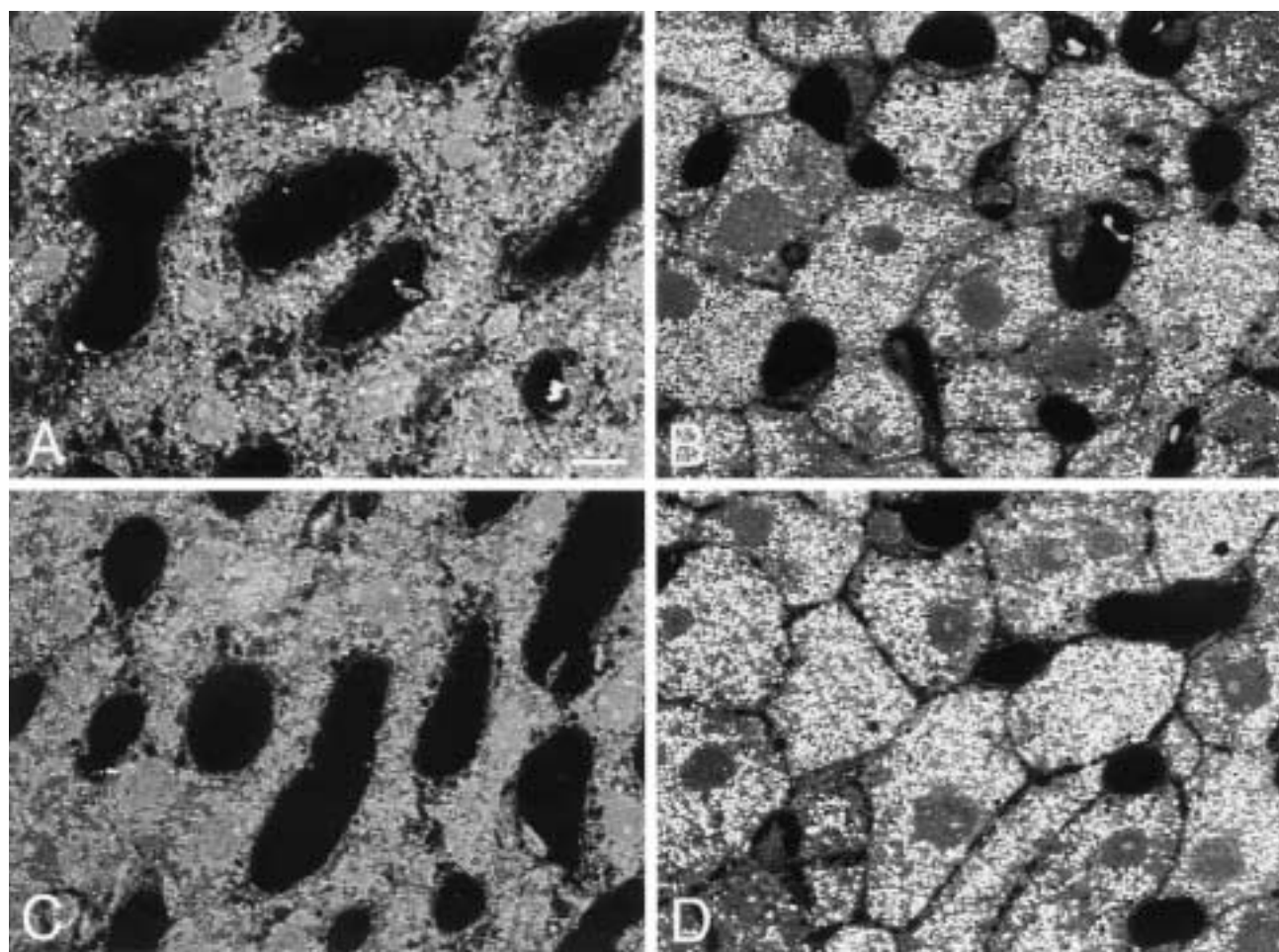

Figure 2 Light micrographs of liver tissues observed by CLSM. Normal (**A,C**) and DOP-treated tissues (**B,D**) stained for catalase (**A,B**) and PH (**C,D**) by the protein A–gold technique. The intensity of reflection varies among groups. Bar = 10 μm.

sured. The same measurement condition as in normal hepatocytes stained for catalase was applied to the other three kinds of specimens. Control staining was performed using the IgG fraction of nonimmune serum instead of antibodies.

Effect of Antibody Concentration

Another experiment was carried out to determine the effect of the concentration of the antibody on the relationship between the data of the two procedures: measurement with electron microscopy and that with CLSM. Serial sections of DOP-treated liver tissue were stained for both procedures as described above with various concentrations of anti-catalase antibody, 0.32, 1.6, 8, and 40 μg/ml of IgG.

Statistical Analysis

Data obtained by immunoelectron microscopy and by CLSM were statistically analyzed by analysis of variance (ANOVA) and the differences between respective groups were judged to be significant at $p < 0.05$.

Results and Discussion

In the observations using CLSM, an increase in the number of peroxisomes was evident in the DOP-treated hepatocytes compared with normal hepatocytes (Figure 2). In addition, the difference in the intensity of the reflection from peroxisomes could be recognized in the four groups by careful observation. A small number of intense light reflections were observed over normal hepatocytes stained for catalase (Figure 2A), and many but less intense reflections were observed over DOP-treated hepatocytes (Figure 2B). A small number of light reflections were observed over normal hepatocytes stained for PH (Figure 2C). However, the observation was difficult because of the weakness of light reflections. Many intense light reflections were observed over DOP-treated hepatocytes (Figure 2D). On electron microscopic observation, peroxisomes of normal hepatocytes stained for catalase by the protein A–gold technique were densely labeled with gold particles (Figure 3A) but those of DOP-treated hepatocytes were less so (Figure 3B). Staining of peroxisomes of normal hepatocytes for PH was rather weak (Figure 3C) but those of DOP-treated hepatocytes were densely labeled (Figure 3D).

The labeling density for peroxisomes calculated on electron micrographs and the intensity of light reflection from peroxisomes measured by CLSM are summarized in Figure 4. The intensity levels of light reflections measured by CLSM for the four were in the following order: normal peroxisomes stained for catalase; DOP-treated peroxisomes stained for PH; DOP-treated peroxisomes stained for catalase; and normal

peroxisomes stained for PH (Figure 4A). The labeling densities for the four groups calculated on electron micrographs were in the same order (Figure 4B). The labeling density on electron microscopic observation and the intensity of light reflection by CLSM were in a good mutual relationship, approximately in a line (Figure 4C). A similar comparison of the data from these two procedures was made on another measurement employing serial sections of DOP-treated hepatocytes stained for catalase with various concentrations of the antibody. The labeling density and the intensity of the light reflection were ordered according to the concentration of the antibody. These two were also well correlated with high concentrations of the antibody, but the value for the lowest (0.32 μg/ml) appeared not to be within the linear range (Figure 5).

As a way of estimating the changes in the total amount of antigens on electron microscopic specimens stained by the protein A–gold technique, the total labeling index or immunolabeled concentration (Nemali et al. 1988), i.e., volume density × labeling density, has been employed. A similar estimate was made with CLSM, defining the total labeling index for CLSM as volume density × the intensity of light reflection. An increase in the amount of peroxisome enzymes, in the form of a moderate increase for catalase and a marked
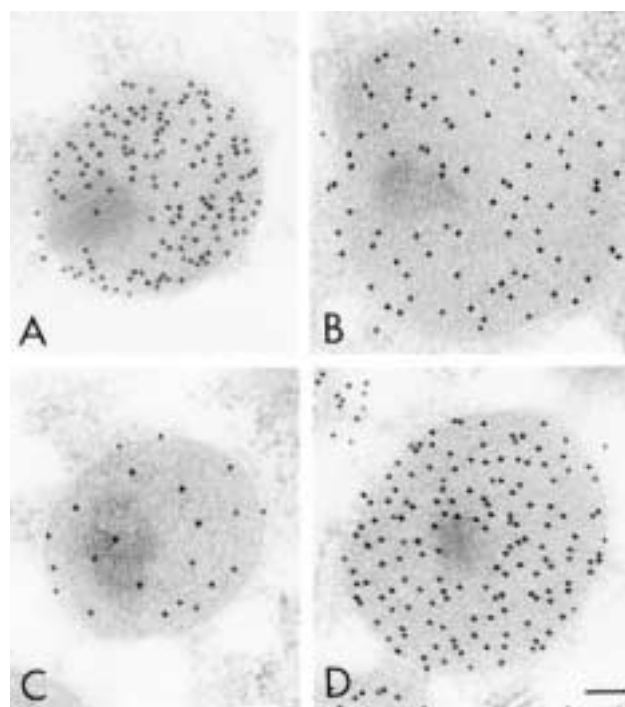

Figure 3 Electron micrographs of hepatic peroxisomes of normal (**A,C**) and DOP-treated rats (**B,D**) stained for catalase (**A,B**) and PH (**C,D**) by the protein A–gold technique. Bar = 0.1 μm.

Figure 4 Values measured in peroxisomes by CLSM (**A**) and the labeling densities of peroxisomes by immunoelectron microscopy (**B**) and of normal (NL) and DOP-treated (DOP) hepatic peroxisomes stained for catalase (CAT) (40 μg/ml of IgG) and enoyl-CoA hydratase/3-hydroxy acyl-CoA dehydrogenase (PH) (40 μg/ml of IgG) by the protein A–gold technique. Values (shown as means ± SE) are significantly different (*p*<0.05) among all groups by ANOVA in each procedure. (**C**) Correlation of the values obtained by the two procedures.
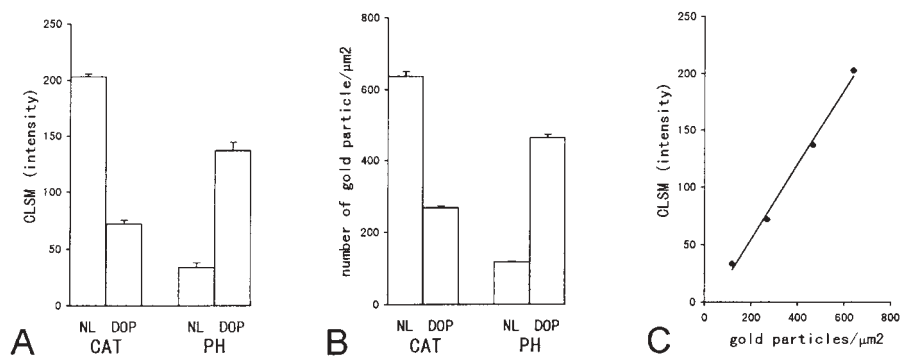
increase for PH, was obtained (Table 1). Similarly to the quantification analysis using electron micrographs, quantification by CLSM also revealed an increase in the volume density of peroxisomes and a change in the labeling indices for peroxisomal enzymes (a decrease for catalase and an increase for PH) induced by administration of a peroxisome proliferator. Just as the total labeling indices obtained by the quantification of electron microscopic pictures for both enzymes increased, the labeling index for CLSM also showed an increase. These changes in volume density, labeling density, and labeling index were similar to the data obtained with other kinds of peroxisome proliferators (Beier et al. 1988; Nemali et al. 1988; Beier and Fahimi 1992).

There are several representative immunoelectron microscopic techniques. The immunogold techniques include the protein A–gold technique, the ferritin tech-

nique, and the immunoperoxidase technique. The immunogold technique has various advantages because of the particulate and electron-dense reaction products of colloidal gold particles; the ultrastructure behind the gold particles is clearly visible and a higher resolution of the picture is obtainable than with other techniques. Another advantage is quantification of the particles for estimating the amount of antigen in the fine structure, i.e., the number or density of gold particles correlates with the amount of antigen (Griffiths 1993). It is possible to determine the relative concentration of antigens in each ultrastructure (Bendayan et al. 1980), including those in substructures in cell organelles (Usuda et al. 1990,1991a,b), by counting the number of gold particles and calculating the labeling density. The difference in the relative concentration of antigens in the ultrastructure, particularly among various experimental groups, can be estimated, e.g., the changes due to aging (Desjardins and Bendayan 1991; Johkura et al. 1998) and the change in localization or
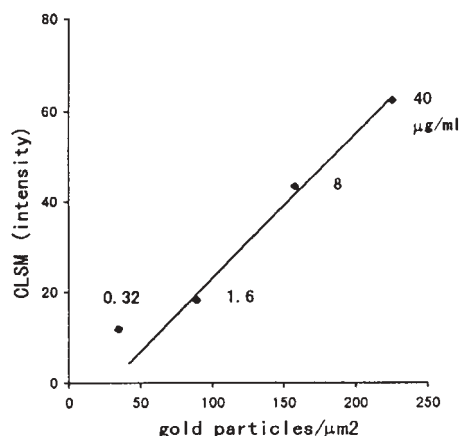
Figure 5 The relationship between the labeling densities on immunoelectron microscopy and the values measured by CLSM on peroxisomes. DOP-treated liver tissues were stained with various concentrations of anti-catalase antibody (0.32, 1.6, 8, and 40 μg/ml of IgG) employing the protein A–gold technique.

Table 1 Changes (the ratio of DOP to control) in the volume density of peroxisomes, labeling density or intensity of light reflection, and total labeling index of catalase and PH on DOP administration[a]

	Volume density	Ratio DOP:control labeling density or intensity of light reflection		Total labeling index	
		CAT	PH	CAT	PH
CLSM	7.27	0.39	5.45	2.83	39.4
EM	7.06	0.42	3.94	2.96	27.8

[a]Volume density was obtained by the ratio of the area of peroxisomes in the cytoplasm of hepatocytes. The labeling density for electron microscopy (EM) of peroxisomes stained for catalase (CAT) and enoyl-CoA hydratase/3-hydroxyacyl-CoA dehydrogenase (PH) by protein A–gold is the number of gold particles in the area of peroxisomes (μm^2). The intensity of light reflection for confocal laser scanning microscope (CLSM) is the intensity of light reflection from peroxisomes. The total labeling indices were calculated as volume density × intensity of light reflection for CLSM observation and volume density × labeling density for EM observation. The ratios of the values for dioctyl-phthalate (DOP)-treated and normal hepatocytes are shown.

movement of antigens resulting from experimental conditions and disease (Makino et al. 1993). DOP, a plasticizer employed in the present study, is well known for causing remarkable changes in the amount of various peroxisomal enzymes. The protein A–gold technique has been used to demonstrate changes in the ultrastructure of peroxisomes and in the matrix enzymes and membrane polypeptides (Bendayan and Reddy 1982; Nemali et al. 1988; Usuda et al. 1988,1991b; Baumgart et al. 1989).

Although the immunogold technique has ordinarily been used for electron microscopy, it can also be used for light microscopic observation without any intensification, thanks to the CLSM (Van den Pol 1989). There are a number of advantages to the observation by CLSM of specimens stained by the protein A–gold technique. Because a wider area can be observed by CLSM than by electron microscopy and the reflection light in CLSM is intense, the distribution of the antigens or immunoreactive cell organellae can be visualized over the whole tissue area. As the labeling density and the total labeling index of gold particles observed by electron microscopy correlated with the light reflection and the total labeling index observed by CLSM as presented in this study, those by CLSM can indicate the relative amount of the antigen. The labeling index reflects the total amount of the antigen. The CLSM has also been employed on specimens stained by the immunofluorescent technique to estimate the amount of antigen (Good et al. 1992; Larsen et al. 1994; Verschure et al. 1994). This may be possible in theory but it appears to be impossible in practice owing to the attenuation of the fluorescence during observation. Accordingly, quantification of the reaction products of immunostaining by CLSM should be done on specimens stained not by the immunofluorescent technique but by the protein A–gold technique, in which attenuation of the reflection light never occurs. Observation by CLSM of cell organelles and quantification of the reaction products on specimens stained by the protein A–gold technique, of course need to be done side by side with electron microscopic observation because CLSM can not recognize the ultrastructure needed to distinguish the kinds of immunoreactive cell organelles.

In the observation of specimens stained by the protein A–gold technique, the change in the labeling density of gold particles shown by electron microscopic observation correlates with the change in the reflection intensity measured by CLSM observation, which is especially suitable for specimens densely labeled by protein A–gold particles. Because a wider area of specimens can be observed by CLSM than by electron microscopy, a highly reliable estimate of the amount of antigens in the tissues stained by the protein A–gold technique is possible by CLSM observation combined with electron microscopy.

Literature Cited

Asaka Y, Watanabe J, Kanamura S (1998) Localization of xenobiotic-responsive element binding protein in rat hepatocyte nuclei after methylcholanthrene administration as revealed by in situ Southwestern hybridization. J Histochem Cytochem 46:825–832

Baumgart E, Völkl A, Hashimoto T, Fahimi HD (1989) Biogenesis of peroxisomes: immunocytochemical investigation of peroxisomal membrane proteins in proliferating rat liver peroxisomes and in catalase-negative membrane loops. J Cell Biol 108:2221–2231

Beier K, Fahimi HD (1985) Automatic determination of labeling density in protein A–gold immunocytochemical preparations using an image analyzer. Histochemistry 82:99–100

Beier K, Fahimi HD (1992) Application of automatic image analysis for quantitative morphological studies of peroxisomes in rat liver in conjunction with cytochemical staining with 3-3'-diaminobenzidine and immunocytochemistry. Microsc Res Tech 21:271–282

Beier K, Völkl A, Hashimoto T, Fahimi HD (1988) Selective induction of peroxisomal enzymes by the hypolipidemic drug bezafibrate. Detection of modulations by automatic image analysis in conjunction with immunoelectron microscopy and immunoblotting. Eur J Cell Biol 46:383–393

Bendayan M (1984) Protein A–gold electron microscopic immunocytochemistry: methods, applications and limitations. J Electron Microsc Tech 1:243–270

Bendayan M, Reddy JK (1982) Immunocytochemical localization of catalase and heat-labile enoyl-CoA hydratase in the livers of normal and peroxisome proliferator-treated rats. Lab Invest 47:364–369

Bendayan M, Reddy MK, Hashimoto T, Reddy JK (1983) Immunocytochemical localization of fatty acid metabolizing heat-stable and heat-labile enoyl-coenzyme A (CoA) hydratases in liver and renal cortex. J Histochem Cytochem 31:509–516

Bendayan M, Roth J, Perrelet A, Orci L (1980) Quantitative immunocytochemical localization of pancreatic secretory proteins in subcellular compartments of the rat acinar cell. J Histochem Cytochem 28:149–160

Danscher G, Nörgaard JOR (1983) Light microscopic visualization of colloidal gold on resin-embedded tissue. J Histochem Cytochem 31:1394–1398

de Duve C, Baudhuin P (1966) Peroxisomes (microbodies and related particles). Physiol Rev 46:323–357

Desjardins M, Bendayan M (1991) Ontogenesis of glomerular basement membrane: structural and functional properties. J Cell Biol 113:689–700

Fahimi HD (1969) Cytochemical localization of peroxidatic activity of catalase in rat hepatic microbodies (peroxisomes). J Cell Biol 43:275–288

Faulk WP, Taylor GM (1971) An immunocolloid method for the electron microscope. Immunochemistry 8:1081–1083

Freire M, Boyde A (1990) Study of Golgi-impregnated material using the confocal tandem scanning reflected light microscope. J Microsc 158:258–290

Furuta S, Hayashi H, Hijikata M, Miyazawa S, Osumi T, Hashimoto T (1986) Complete nucleotide sequence of cDNA and deduced amino acid sequence of rat liver catalase. Proc Natl Acad Sci USA 83:313–317

Good MJ, Hage WJ, Mummery CL, de Laat SW, Boonstra J (1992) Localization and quantification of epidermal growth factor receptors on single cells by confocal laser scanning microscopy. J Histochem Cytochem 40:1353–1361

Griffiths G (1993) Quantitative aspects of immunocytochemistry. In Griffiths G, ed. Fine Structure Immunocytochemistry. Berlin, Springer-Verlag, 371–445

Hashimoto T (1996) Peroxisomal β-oxidation: enzymology and molecular biology. Ann NY Acad Sci 804:86–98

Hess R, Stäubli W, Riess W (1965) Nature of the hepatomegalic effect produced by ethyl-chlorophenoxy-isobutyrate in the rat. Nature 208:856–858

Holgate CS, Jackson P, Cowen PN, Bird CC (1983) Immunogold-silver staining: new method of immunostaining with enhanced sensitivity. J Histochem Cytochem 31:938–944

Ito Y, Otsuki Y (1998) Localization of apoptotic cells in the human epidermis by an in situ DNA nick end-labeling method using confocal reflectant laser microscopy. J Histochem Cytochem 46:783–786

Johkura K, Usuda N, Liang Y, Nakazawa A (1998) Immunohistochemical localization of peroxisomal enzymes in developing rat kidney tissues. J Histochem Cytochem 46:1161–1173

Larsen TH, Hesketh JE, Rotevatn S, Greve G, Sætersdal T (1994) Ribosome distribution in normal and infarcted rat hearts. Histochem J 26:79–89

Makino H, Yamasaki Y, Haramoto T, Shikata K, Hironaka K, Ota Z, Kanwar YS (1993) Ultrastructural changes of extracellular matrices in diabetic nephropathy revealed by high resolution scanning and immunoelectron microscopy. Lab Invest 68:45–55

Nemali MR, Usuda N, Reddy MK, Oyasu K, Hashimoto T, Osumi T, Rao MS, Reddy JK (1988) Comparison of constitutive and inducible levels of expression of peroxisomal β-oxidation and catalase genes in liver and extrahepatic tissues of rat. Cancer Res 48:5316–5324

Osumi T, Hashimoto T (1979a) Peroxisomal β-oxidation system of rat liver. Copurification of enoyl-CoA hydratase and 3-hydroxyacyl-CoA dehydrogenase. Biochem Biophys Res Commun 89:580–584

Osumi T, Hashimoto T (1979b) Subcellular distribution of the enzymes of the fatty acyl-CoA β-oxidation system and their induction by di (2-ethylhexyl) phthalate in rat liver. J Biochem 85:131–139

Reddy MK, Qureshi SA, Hollenberg PF, Reddy JK (1981) Immunochemical identity of peroxisomal enoyl-CoA hydratase with the peroxisome-proliferation-associated 80,000 mol wt polypeptide in rat liver. J Cell Biol 89:406–417

Robinson JM, Batten BE (1989) Detection of diaminobenzidine reactions using scanning laser confocal reflectance microscopy. J Histochem Cytochem 37:1761–1765

Robinson JM, Batten BE (1990) Localization of cerium-based reaction products by scanning laser reflectance confocal microscopy. J Histochem Cytochem 38:315–318

Romano EL, Romano M (1977) Staphylococcal protein a bound to colloidal gold: a useful reagent to label antigen-antibody sites in electron microscopy. Immunochemistry 14:711–715

Roth J (1982) Applications of immunocolloids in light microscopy.

Preparation of protein A-silver and protein A–gold complexes and their application for localization of single and multiple antigens in paraffin sections. J Histochem Cytochem 30:691–696

Roth J, Bendayan M, Carlemalm E, Villiger W, Garavito M (1981) Enhancement of structural preservation and immunocytochemical staining in low temperature embedded pancreatic tissue. J Histochem Cytochem 29:663–671

Roth J, Bendayan M, Orci L (1978) Ultrastructural localization of intracellular antigens by the use of protein A–gold complex. J Histochem Cytochem 26:1074–1081

Sun XJ, Tolbert LP, Hildebrand JG, Meinertzhagen IA (1998) A rapid method for combined laser scanning confocal microscopic and electron microscopic visualization of biocytin or neurobiotin-labeled neurons. J Histochem Cytochem 46:263–273

Uriel J, Lorenzo HK, Macho A, de Feijter AW, Mishal Z (1995) Visualization of silver-enhanced reaction products from protein- and immuno-colloidal gold probes by laser scanning confocal microscopy in reflection mode. Histochemistry 103:355–361

Usuda N, Kuwabara T, Ichikawa R, Hashimoto T, Nagata T (1991a) Immunoelectron microscopic evidence for organ differences in the composition of peroxisome-specific membrane polypeptides among three rat organs: liver, kidney, and small intestine. J Histochem Cytochem 39:1357–1366

Usuda N, Ma H, Hanai T, Yokota S, Hashimoto T, Nagata T (1990) Immunoelectron microscopy of tissues processed by rapid freezing and freeze-substitution fixation without chemical fixatives: application to catalase in rat liver hepatocytes. J Histochem Cytochem 38:617–623

Usuda N, Reddy MK, Hashimoto T, Rao MS, Reddy JK (1988) Tissue specificity and species differences in the distribution of urate oxidase in peroxisomes. Lab Invest 58:100–111

Usuda N, Yokota S, Ichikawa R, Hashimoto T, Nagata T (1991b) Immunoelectron microscopic study of a new D-amino acid oxidase-immunoreactive subcompartment in rat liver peroxisomes. J Histochem Cytochem 39:95–102

Van den Pol AN (1989) Neuronal imaging with colloidal gold. J Microsc 155:27–59

Verschure PJ, van Marle J, Joosten LAB, van den Berg WB (1994) Localization and quantification of the insulin-like growth factor-1 receptor in mouse articular cartilage by confocal laser scanning microscopy. J Histochem Cytochem 42:765–773

Woolf NK, Jaquish DV, Koehrn FJ, Woods VL, Peterson DA (1996) Improved resolution of fibronectin mRNA expression in the inner ear using laser scanning confocal microscopy. J Histochem Cytochem 44:27–34

Yokota S, Völkl A, Hashimoto T, Fahimi HD (1987) Immunoelectron microscopy of peroxisomal enzymes: their substructural association and compartmentalization in rat kidney peroxisomes. In: Fahimi HD, Sies H, eds. Peroxisomes in Biology and Medicine. Berlin Heidelberg, Springer-Verlag, 115–127